Published as: *Nature*. 2014 November 13; 515(7526): 269–273.

The participation of cortical amygdala in innate, odor-driven behavior

Cory M. Root[1], **Christine A. Denny**[2,3,4], **René Hen**[3,4,5], and **Richard Axel**[1]

[1] Department of Neuroscience and the Howard Hughes Medical Institute, College of Physicians and Surgeons, Columbia University, New York, NY 10032 USA

[2] Department of Biological Sciences, New York State Psychiatric Institute, New York, NY 10032, USA

[3] Department of Neuroscience and Psychiatry, New York State Psychiatric Institute, New York, NY 10032, USA

[4] Division of Integrative Neuroscience, New York State Psychiatric Institute, New York, NY 10032, USA

[5] Department of Pharmacology, Columbia University, New York State Psychiatric Institute, New York, NY 10032, USA

Abstract

Innate behaviors are observed in naïve animals without prior learning or experience, suggesting that the neural circuits that mediate these behaviors are genetically determined and stereotyped. The neural circuits that convey olfactory information from the sense organ to the cortical and subcortical olfactory centers have been anatomically defined[1-3] but the specific pathways responsible for innate responses to volatile odors have not been identified. We have devised genetic strategies that demonstrate that a stereotyped neural circuit that transmits information from the olfactory bulb to cortical amygdala is necessary for innate aversive and appetitive behaviors. Moreover, we have employed the promoter of the activity-dependent gene, *arc*, to express the photosensitive ion channel, channelrhodopsin, in neurons of the cortical amygdala activated by odors that elicit innate behaviors. Optical activation of these neurons leads to appropriate behaviors that recapitulate the responses to innate odors. These data indicate that the cortical amygdala plays a critical role in the generation of innate odor-driven behaviors but do not preclude the participation of cortical amygdala in learned olfactory behaviors.

Corresponding author Correspondence to: Richard Axel.

Contributions

C.M.R. and R.A. conceived the project, participated in its development, wrote the manuscript and analyzed data. C.M.R. performed all experiments. C.A.D. and R.H. conceived and generated the ArcCreER^{T2} transgenic mouse.

Competing financial interests

The authors declare no competing financial interests.

Odors can elicit an array of innate behaviors including feeding, mating, freezing or escape, responses essential for the survival and reproduction of the organism. Innate responses to odors can be mediated by either the vomeronasal or main olfactory system[4]. The vomeronasal organ recognizes non-volatile odorants, including the major urinary proteins[5] and steroids[6], that elicit innate responses via a circuit emanating from the accessory olfactory bulb. The main olfactory system recognizes volatile cues including 2, 3, 5-trimethyl-3-thiazoline (TMT) in fox secretions[7] and trace amines in bobcat[8] and mouse[9] urine that elicit innate attraction and avoidance responses.

Olfactory perception is initiated by the recognition of odorants by a large repertoire of receptors in the sensory epithelium[10-12]. Neurons expressing a given receptor are randomly distributed within zones of the epithelium but project with precision to two spatially invariant glomeruli in the olfactory bulb[13-15]. Thus a transformation in the representation of olfactory information is apparent in the bulb where the dispersed population of active neurons in the sense organ is consolidated into a discrete spatial map of glomerular activity[16]. This invariant glomerular map in the bulb is transformed in the representations in higher olfactory centers. Anatomic tracing experiments reveal that the projections from the olfactory bulb to the cortical amygdala retain a topographic map with individual glomeruli projecting to broad but spatially invariant loci[1]. In contrast, spatial order in the bulb is discarded in the piriform cortex; axons from individual glomeruli project diffusely to the piriform cortex without apparent spatial preference[1-3]. The identification of a distributive pattern of projections to the piriform cortex and stereotyped projections to the cortical amygdala provides an anatomical substrate for the generation of learned and innate behaviors. We have devised behavioral assays and genetic strategies to identify the olfactory centers responsible for innate odor-driven behaviors.

Innate behaviors are often complex and are comprised of multiple components, but can be simplified by the design of assays that categorize behaviors by only a single axis, positive or negative valence. We therefore developed an open field behavioral assay to determine whether a given odor elicits attraction or avoidance as a measure of innate odor valence. A symmetrical chamber was constructed with four quadrants allowing independent airflow into each of the quadrants with a vacuum in the center. In the absence of odor, mice explored the chamber without bias for any quadrant (Extended Data Fig. 1f). However, the addition TMT to one quadrant results in significant avoidance (Fig. 1a and Extended Data Fig. 1).

We describe the valence of behavioral response to an odor by defining a performance index (PI: see Legend to Fig. 1), such that a negative value indicates avoidance and a positive value indicates attraction. In this behavioral assay, TMT reveals a PI of −83±5.0 (n=5). TMT not only elicits avoidance, but also sitting in distant quadrants, resulting in a marked decrease in locomotor activity, which may be a proxy for freezing (Extended Data Fig. 1e,h). This behavioral assay was employed to examine the response of mice to several odorants. We observe that a small group of odorants elicit reliable approach or avoidance behavior, but most odors elicit no significant behavioral response (Fig. 1b). For example, peanut oil and 2-phenylethanol, a component of rose oil, elicits attraction (PI of 50±4.1 and 49±4.8 (n=5) respectively), whereas the odorants TMT, isopentalamine and 4-

methylthiazole elicit aversion (PI −83±5.0, of −81±4 and −59±8.1 (n=4) respectively. Most odors are neutral in this assay and reveal PIs near zero ranging from −7 to 9. Therefore, this robust assay is able to classify the innate valence of odors in terms of approach and avoidance responses.

We have used this behavioral assay in concert with optogenetic silencing to identify a higher olfactory center necessary for innate olfactory-driven behaviors. The mitral and tufted cells of the olfactory bulb project axons to at least five brain regions[1]: piriform cortex, cortical amygdala, entorhinal cortex, accessory olfactory nucleus, and olfactory tubercle. We expressed the light-activated chloride pump, halorhodopsin[17], in neurons of the olfactory bulb to permit optical silencing of the individual projections to these olfactory centers and examined the consequences on innate odor-driven behaviors.

Bilateral injection of an adeno-associated virus (AAV) encoding halorhodopsin fused to eYFP (AAV-syn-eNpHR3.0-eYFP) results in expression in the vast majority of mitral cells in the olfactory bulb (80%±7 SD; Fig. 2a,b). Intrinsic neurons within the bulb also express halorhodopsin-eYFP, but mitral and tufted cells provide the only feed-forward excitatory output to cortical centers. In initial experiments, we asked whether silencing of neurons within the olfactory bulb suppressed the innate behavior elicited by TMT. After bilateral infection, both olfactory bulbs were illuminated by introducing optical fibers coupled to a 561nm laser above the dorsal surface of the bulb. Previous experiments suggest that the glomeruli responsible for innate behavior are restricted to the dorsal bulb[7]. Mice were then introduced into the behavioral chamber in which TMT was present within one quadrant and innate aversion was examined in the absence or presence of 561nm illumination to silence bulbar activity. We observed that light-activated silencing of the olfactory bulb significantly suppressed the aversion to TMT with a reduction in the PI from −82±3.8 to −18±2.9 (n=3). These experiments demonstrate that these viral injections into the bulb result in halorhodopsin expression in neurons essential for innate aversive behavior.

We then employed optical silencing of the individual targets[18] of the olfactory bulb to identify the olfactory centers necessary to elicit innate behavior. Photostimulation of the cortical amygdala (Extended Data Fig. 2), for example, in mice expressing halorhodopsin in bulbar neurons should selectively silence bulbar input to this brain structure without affecting input to other olfactory centers. Mice were coupled to a 561nm laser and were placed in the four-field behavioral assay with TMT in a single quadrant. Each of eleven mice exhibited a striking reduction in the avoidance of the TMT quadrant upon bilateral illumination of the cortical amygdala (PI= −65±3.4 without photostimulation, and −7.9±8.4 upon optical silencing) (Fig. 2d). Further, silencing bulbar input significantly reduced the freezing behavior as evidenced by decreased bouts of inactivity (Extended Data Fig. 3). The inhibition of innate avoidance observed upon optical silencing of the cortical amygdala was reversible; robust avoidance re-emerged upon cessation of light-induced silencing (PI= −74±5.7). In control animals not injected with virus, aversive behavior was not impaired by photostimulation (Fig. 2f). We determined the efficacy of silencing upon illumination of bulbar axons by analyzing c-fos activity. We observe a 70% reduction in the frequency of cells activated by odor in cortical amygdala but not olfactory tubercle or piriform cortex (Extended Data Fig. 4). These results demonstrate that axonal silencing is sufficient and

suggests that antidromic hyperpolarization is not responsible for the suppression of behavior.

We next determined whether input from the olfactory bulb to cortical amygdala is also required for innate attraction. We observe that light-induced silencing of olfactory input to cortical amygdala eliminates attraction to 2-phenylethanol (PI without photostimulation, 48±3.2; PI with photostimulation, −8.3±2.1) (Fig. 2e,g; Extended Data Fig. 3b,d), but attraction resumes upon cessation of optical silencing. Thus, input from the olfactory bulb to the cortical amygdala is required to elicit innate responses to both appetitive and aversive odors.

We also asked if suppression of olfactory input to either piriform cortex or olfactory tubercle, two additional targets of the bulb, would suppress innate, odor-driven behaviors. Bilateral illumination of axons from the olfactory bulb to either the tubercle or the piriform failed to suppress the innate aversion to TMT (PI: −61±3.4 and −67±4.0, respectively, n=7 & 8) (Fig. 2f). Conclusions from these experiments, however, must be tempered by the fact that olfactory inputs to both the tubercle and piriform are extensive and the area of illumination might have been inadequate to significantly suppress axonal input. Nonetheless, this result provides an additional control for antidromic suppression of mitral and tufted cell activity that would result in suppression of innate behavior independent of the site of optical silencing.

These observations predict that silencing of neurons intrinsic to the cortical amygdala should also inhibit innate behavior. Halorhodopsin was therefore expressed in the neurons of the cortical amygdala after bilateral injections of AAV-eNpHR3.0-eYFP and bilaterally implanted optical fibers (Extended Data Fig. 5). In each of five mice, we observed a significant decrease in aversion of the TMT quadrant in the four-field behavioral assay (PI prior to stimulation, −70±4.8; after photostimulation, −15±7.1) (Fig. 2f). Thus, light-induced silencing of the olfactory bulb, the bulbar projections to cortical amygdala, or the neurons of the cortical amygdala dramatically impairs innate aversion to TMT.

Our data suggest that distinct cell populations that reside within the cortical amygdala are capable of eliciting innate responses to either appetitive or aversive odors. We next identified and manipulated the activity of these neurons by exploiting the promoter of the activity-dependent gene, *arc*[19], to drive the expression of the light activated cation channel, channelrhodopsin[20]. AAV encoding a Cre-dependent channelrhodopsin fused to the fluorescent protein eYFP (AAV-ef1α-DIO-ChR2-eYFP) was injected into the cortical amygdala of mice harboring a transgene in which the *arc* promoter drives the expression of the tamoxifen-sensitive Cre-recombinase ($CreER^{T2}$) (Fig. 3a). In this $ArcCreER^{T2}$ mouse[21], neuronal activation should result in the expression of $CreER^{T2}$. In the presence of tamoxifen, activated Cre will effect the recombination between the loxP sites of AAV-ef1α-DIO-ChR2, resulting in the irreversible expression of ChR2-eYFP. The fusion of Cre with the tamoxifen-sensitive estrogen receptor allows for temporal control of the recombination activity. Thus administration of tamoxifen followed by exposure to odor should result in the expression of ChR2-eYFP in the neurons activated by the odor (Fig. 3b,c), permitting us to mark and manipulate the activity of these neural populations.

In initial experiments, we determined whether ChR2-eYFP is faithfully expressed in neurons that respond to specific odors in the cortical amygdala. ChR2-eYFP should be expressed by neurons responsive to TMT and subsequent re-exposure of the mice to TMT should result in the acute expression of endogenous arc in ChR-eYFP positive neurons. This temporal separation permitted us to identify populations of neurons activated by sequential stimuli in the same animal and allowed us to determine whether the expression of ChR2-eYFP is a faithful reporter of endogenous *arc* activity. We observe that 80% ± 5.9 (SD) of the ChR2-eYFP+ neurons also express endogenous arc (n=4). About 50% of the neurons expressing endogenous arc also express ChR2-eYFP (Extended Data Fig. 6a,c). These results indicate that the expression of ChR2-eYFP is a faithful reporter of endogenous *arc* activity, identifying a population of neurons responsive to TMT.

We next asked whether odors that elicit innate behaviors of different valence activate different populations of neurons in the cortical amygdala. AAV encoding Cre-dependent ChR2 was injected into the cortical amygdala of ArcCreER^{T2} mice. After tamoxifen treatment, the mice were sequentially exposed to the attractive odor, 2-phenylethanol and the aversive odor, TMT. In this experimental design, the neurons responsive to 2-phenylethanol will express ChR2-eYFP, whereas the neurons responsive to TMT will express the endogenous arc. Only 4% ± 2.1 (SD) of the ChR2-eYFP+ neurons activated by 2-phenylethanol also express endogenous arc, activated by TMT (n=4) (Extended Data Fig. 6b,c). These data suggest that odors that elicit appetitive and aversive innate behaviors activate different populations of neurons in the cortical amygdala that can be faithfully identified and manipulated following AAV infection of an ArcCreER^{T2} mouse.

The ArcCreER^{T2} mice were used to determine whether the cortical amygdala is sufficient to elicit a response that recapitulates the behavior observed with odor. We therefore injected AAV encoding Cre-dependent ChR2-eYFP into the cortical amygdala of ArcCreER^{T2} mice and optical fibers were implanted unilaterally above the injection site. Mice were treated with tamoxifen and then exposed to odor. We observe ChR2 expression in cortical amygdala and neighboring areas of piriform cortex and medial amygdala. However, c-fos staining demonstrates that optical activation is restricted to cortical amygdala as a consequence of fiber placement (Extended Data Fig. 7). Behavioral assays were performed in the four-field arena, but odor was not placed in one quadrant, rather the entrance to a single quadrant triggered pulsed laser stimulation via a custom closed loop computer program.

Photoactivation of the cortical amygdala of mice expressing ChR2 after TMT exposure, resulted in avoidance of the optically stimulated quadrant (PI of −49±4.6, n=6) (Fig. 3d) and increased freezing as evidenced by increased immobility (Extended Data Fig. 8). In contrast, mice expressing ChR2 in neurons responsive to the innately attractive odor, 2-phenylethanol, exhibited significant attraction to the quadrant in which the mice received optical stimulation (PI of 42±6.4, n=4) (Fig. 3f). Mice expressing channelrhodopsin in neurons responsive to the neutral odor, isoamyl acetate, did not exhibit any discernible behavioral response upon optical stimulation (PI of 5.6±8.6, n=6) and explored each quadrant equally (Fig. 3e). In control mice, treatment with tamoxifen without odor exposure resulted in ChR2 expression in a very small subpopulation of neurons. These mice did not exhibit any behavioral bias upon photostimulation within a single quadrant (PI of −5.2±7.1,

n=3) (Fig. 3g). These experiments demonstrate that odors that elicit innate behaviors of different valence activate different populations of neurons within the cortical amygdala. Moreover, photoactivation of these two distinct populations of neurons is sufficient to elicit an appropriate behavioral response. Thus, these neural representations reflect an essential component in a determined neural circuit wired to elicit an innate behavioral response to odors.

The presence of spatially stereotyped projections from individual glomeruli to the cortical amygdala[1] suggest that the neural representations activated by aversive and attractive odors may be anatomically segregated. We therefore examined the spatial distribution of neurons activated by odor after AAV infection of the ArcCreER^{T2} mouse (Fig. 4a,b and Extended Data Fig. 9). We observe that the distribution of ChR2-eYFP^{+} neurons, activated by the appetitive odors, 2-phenylethenol and peanut oil, are most abundant in the caudal third of the posterolateral cortical amygdala. Sparse labeling is observed in more anterior regions. In contrast, the aversive odors, TMT, isopentylamine and 4-methylthiozoline activate neurons distributed throughout the cortical amygdala. Significant labeling is observed in more anterior regions that are not activated by odors that elicit appetitive behaviors. Neutral odors, such as isoamyl acetate also fail to activate neurons in the anterior region and reveal labeling in a pattern not dissimilar from that observed with appetitive odors.

A given odor, even those that elicit innate behaviors, may activate as many as 100 glomeruli and the inputs from these glomeruli may activate neurons distributed diffusely across the cortical amygdala. Neurons in the most anterior portion of the cortical amygdala, however, may only be activated by odors that elicit innate aversive behaviors. Our data suggest a model in which aversive odors activate a small subset of glomeruli that project to anterior cortical amygdala and a larger set of glomeruli that project more broadly throughout the cortical amygdala. Regions responsible for appetitive behaviors may reside in more posterior domains, however a locus that is uniquely responsive to appetitive odors is not easily distinguishable in our analyses. Neurons in the cortical amygdala are also activated by neutral odors that do not elicit an apparent behavioral response. We do not know the functional significance of the neural representation of neutral odors. These neurons may also reside in segregated domains that encode innate features of an odor, including subtle behaviors or odor quality, that are not discernible in our assays. Alternatively, the neurons in cortical amygdala responsive to neutral odor may participate in the adaptive response to odors, a function thought to engage the piriform cortex[22].

The response to most odors is not innate but adaptive. The majority of odors have predictive value only over the lifetime of the organism and acquire meaning through learning, a function suited to the unstructured representation in piriform cortex[23-25]. Exogenous activation of an arbitrarily chosen ensemble of piriform neurons can result in appetitive, aversive and social behaviors only after associative learning[22]. Therefore, odor representations in piriform cortex are afforded behavioral significance upon experience. Our data indicate that the cortical amygdala plays a critical role in the generation of innate odor-driven behaviors but do not preclude the participation of cortical amygdala in learned olfactory behaviors. Cortical amygdala may cooperate with piriform cortex to impose meaning on a random ensemble of active neurons in piriform. One major target of piriform

output is the cortical amygdala[26]. Piriform connections in the cortical amygdala may therefore exploit the distinct subpopulations of neurons in cortical amygdala capable of eliciting innate behaviors to generate learned responses to odor. In one model, direct connections from olfactory bulb to cortical amygdala may elicit innate odor-driven behaviors, whereas indirect connections from bulb through piriform to cortical amygdala may elicit learned responses to odor. This indirect, trisynaptic pathway may facilitate learning-dependent synaptic changes necessary to impart valence on a random ensemble of neurons. The convergence of direct monosynaptic input and indirect polysynaptic input, capable of more complex computations, from the same brain structure is a common motif in both vertebrate[27] and invertebrate[28] brains.

ONLINE METHODS

Behavioral assay

The four-field behavior chamber was inspired by similar assays used in experiments with Drosophila (See Methods References[29-31]). The custom behavioral chamber was machined from plastic materials with the help of the Columbia University machine shop on the Nevis Campus. The chamber is an enclosed four-quadrant arena with airflow into the center and a vacuum in the middle. Airflow at 150 mL/min is pumped into each quadrant via gas-mass flow controllers (cole-parmer). Airflow exits the chamber via a 1inch outlet in the center of the floor covered by steel mesh. The outlet is connected a vacuum line with a gas-mass controller set to 700 mL/min. The chamber has a 76 cm diameter, a corner arc of 1.9 cm radius, and a chamber height of 7.6 cm. The floor and the walls are made out of polypropylene and the hinged ceiling is clear, ½” thick acrylic. Odor is applied by solenoid valves redirecting airflow through 100 mL glass bottles containing 1 μL of pure odorant on a small piece of kimwipe. The chamber is housed in a dark environment and illuminated by infrared lights below the floor. A Basler A601FM camera (Edmund Optics) mounted above the chamber records the animal behavior. Custom software written in Labview (National Instruments) tracks the position of the mouse in real time at a rate of 4 Hz. The behavior was further analyzed offline using custom, unbiased scripts written in Igor Pro (Wavemetrics).

Mice were placed in the chamber for 25 min experiments and tested only once per day. The first 10 min serve as a baseline test for bias within the arena. The first two minutes of data after the odor was introduced was excluded from the analysis to reduce variance without affecting the overall valence of the behavioral response. The symmetrical behavior chamber was contained in a lightproof structure and illuminated by infrared lights. Therefore, there were no spatial cues available to the animals with respect to the room, and the odor was always delivered in the same quadrant. To control for any spatial bias, animals were always tested with a 10 min period of no odor. If an animal avoided any one quadrant more than 20% from chance, the experiment was terminated and the animal was tested again on another day. For the experiments in Figure 1, this occurred in less than 10% of the trials and a given animal was never excluded from the data set. For the optogenetic experiments, mice were more inclined to sessions of inactivity resulting in bias for one area during the baseline period. Repeated baseline testing acclimated the animals to being tethered in the chamber, which typically permitted the experiment to proceed after 1 or 2 baseline sessions. About

half of the animals required more than 1 baseline period before the experiment could continue. Of the 65 mice tested in the optogenetic experiments, only 4 were rejected because of unremitting problems with locomotor activity or spatial bias during the baseline period. Moreover, we have observed that a given animal can be retested to the same odor at least 5 times on consecutive days and exhibit no experience-dependent bias during the baseline, and then exhibit reliable responses to the odor (data not shown). Therefore, mice do not exhibit any signs of conditioned place preference or learned responses to odor in this assay. Experiments in Figure 1a-d were performed with the same set of animals, and those in Fig. 1e were obtained from overlapping groups of animals. Odors were tested in random order. A preliminary set of experiments revealed that depending on the variance and magnitude of difference a sample as small as 4 animals was sufficient to achieve significant findings.

Optogentic Behavior experiments

Animals were only tested once per day, and the laser on/off sessions occurred at least one day apart. Half of the mice experienced odor with the laser on upon the first test, and the other half experienced the odor with the laser off first. Mice were implanted with custom-made fiber cannulas assembled as follows. Optical fibers (200 μm, 0.39 NA, Thorlabs) were epoxied to 2.5 mm stainless steel ferrules (Precision Fiber Products), and polished with a fiber optic polishing kit (Thorlabs) to achieve a minimum of 80% transmission. After surgical implantation, the ferrules protruding from an animal's head could be coupled to either a 100 mW 473 nm or 100 mW 561 nm laser (Shanghai Laser & Optics Century) via custom made patch cords with either a single, or beam splitting, rotary joint (Doric Lenses) in between the mouse and the laser. The fiber was introduced to the behavior chamber through a 1 cm hole in the left side of the chamber. During the behavioral experiment, it was necessary to pull the slack of the fiber as the mouse traversed the chamber in order to prevent the mouse from getting tangled in the fiber. Therefore, a motorized pulley system was created to pull the fiber coupled rotary joint along a vertical tract adjacent to the hole where the fiber enters the chamber. Custom closed loop software written in Labview monitored the position of the mouse and drove the pulley system to adjust the height of the rotary joint to maintain the appropriate amount of slack. The blue laser was pulsed with 50 ms bins at 10 Hz, and there was a steep gradient from 1-10 Hz along the perimeter of the quadrant. The lasers were controlled by TTL modulation from custom Labview software.

Light intensity

Fibers were implanted approximately 200-400 μm above layer II of cortical amygdala, which should illuminate an area with a radius no more than 600 μm. For halorhodopsin experiments the 561 nm laser power was adjusted to produce an estimated 10 mW at the implanted fiber tip, which we calculate to provide an irradiance of 9-22 mW/mm^2 at layer II of cortical amygdala. Suppression in the olfactory bulb was performed by placing optical fibers bilaterally 0.5-1 mm above the center of the dorsal surface of the bulb. We estimate the conical spread of light from the fiber tip illuminates an area of about 3.5 mm in diameter with at least 7 mW/mm^2. In these experiments, the fiber was introduced through a bilateral cannula positioned in the center of the olfactory bulbs about 0.5mm above the surface at coordinate relative to bregma (~5.0 AP, 1.0 ML). The olfactory bulb is roughly 3 mm in length and 1-2 mm wide; therefore, fibers placed above the center should illuminate the

most of the dorsal surface. For channelrhopsin experiments the 473 nm laser was adjusted to an estimated 5-7 mW at the implanted fiber tip, which we calculate to provide an irradiance of 7-18 mW/mm^2 at layer II of cortical amygdala. A conservative estimate of the radius of illumination is calculated with trigonometry using the half angle of divergence for a multimode optical fiber: $\theta = sin^{-1}\left(\frac{NA}{n}\right)$ where NA is the numerical aperture of the fiber (0.39) and *n* is the index of refraction of gray matter (1.36)[32]. However, it has been suggested that due to scattering in tissue the lateral spread is quantitatively similar to the depth of forward light spread from the fiber tip[33]. Thus, at 400 μm below the fiber tip the radius of illumination would be 400 μm from the fiber edge. Power attenuation was calculated as described[34]: $\frac{I_z}{I_{z0}} = \frac{\rho^2}{(s_z+1)(z+\rho)^2}$ where $\rho = r\sqrt{\left(\frac{n}{NA}\right)^2 - 1}$ and S_z is the scatter coefficient (11.2) per unit thickness and z is the thickness of the sample.

Experimental subjects

Adult C57BL/6J mice (Jackson laboratory) ages 8-16 weeks old were group housed until surgery and then singly housed on a reverse light cycle. For experiments that did not require surgery, mice were singly housed for at least 5 days prior to testing. ArcCreER^{T2} mice were group housed until 7-9 weeks old when surgeries were performed and then singly housed. In the days preceding behavioral experiments, mice were handled regularly to adapt them to the experimenter and the attachment of fiber patch cords. Halorhodopsin experiments began 3-4 weeks after the viral injection in order to achieve high levels of expression.

Stereotactic surgery

Animals were anaesthetized with ketamine and xylazine (100 mg/kg, 10 mg/kg, respectively, Henry Schein) and placed in a stereotactic frame (Narishige). Small craniotomies were made using standard aseptic technique. Virus was injected with needles pulled from capillary glass (Drummond) at a flow rate of approximately 100 nL/min by manual pressure injection. Each olfactory bulb received two injections of 1 μL of AAV5-hSyn-eNpHR3.0-eYFP (UNC Viral Core) injected in two locations along the AP axis relative to bregma: 5.4 & 6.2 AP, 1.1 ML, −1.4 DV from the bulb surface. Injections into cortical amygdala were also 1 μL in volume at coordinates relative to Bregma: −1.7 AP, 2.8 ML, −5.9 DV. Animals exhibited broad expression covering at least 90% of the area of COApl. For experiments with the ArcCreER^{T2} mice, animals were injected with the Cre-dependent virus: AAV5-ef1α-DIO-hChR2(H134R)-eYFP (UNC Viral Core). Fibers were implanted into the cortical amygdala at about −1.7 AP, 2.8 ML, −5.7 DV for most experiments, but for experiments with photoactivation of ChR2 in 2-phenylethanol responsive neurons the fibers were implanted slightly more posterior (-2.0 AP, 2.9 ML, −5.7 DV). The Fibers were fixed in place using a small amount of clear dental cement (CB Metabond, Parkell, Inc.) covering the surface of the skull, followed by an outer coating of black Ortho Jet dental acrylic (Lang Dental Manufacturing). Buprenorphine (0.05 mg/kg, Henry Schein) was administered. All injection sites and fiber placements were verified histologically and in rare cases mice were excluded if either were mistargeted. All experiments were conducted according to approved protocols at Columbia University.

ArcCreER^{T2} mice

A Transgenic mouse was generated from a Bac clone containing the entire *arc* gene (see[21]). The mice received viral injections at approximately 8 weeks of age. Five days post injection, mice were dark adapted by placing them in a light proof chamber with fresh bedding for 36-48 hours. On day 7 post-injection, mice were administered 2 mg of tamoxifen (Sigma T5648). Tamoxifen was prepared as a 10 mg/mL stock solution dissolved into a 1:10 mixure of ethanol and corn oil (Sigma C8267) and 0.2 mL was administered by IP injection. Six hours after tamoxifen, mice were exposed to odor on a cotton swab placed through the roof of their cage twice for 15 min each during a 1 hour period. 1 μL of pure odorant was pipetted onto the cotton swab. Mice were maintained in the dark for an additional 48 hours after tamoxifen injection before returning to the reverse light cycle. Photoactivation experiments began 3 weeks after tamoxifen and odor exposure.

Histological processing

Mice were administered ketamine and xylazine (100 mg/kg and 10 mg/kg, respectively) and euthanized by transcardial perfusion with 10 mL of PBS, followed by 10 mL of 4% paraformaldehyde in PBS. Brains were extracted and 100 μm coronal sections were cut on a vibratome. The tissue was labeled with the following antibodies: goat anti-GFP (Abcam ab6673), rabbit anti-arc (Synaptic Systems 156-003), goat anti-c-fos (Santa Cruz sc-52-G), alexa-488 donkey anti-goat (Jackson ImmunoResearch), alexa-568 donkey anti-rabbit (Life Technologies A11057), alexa-647 donkey anti-rabbit (Jackson ImmunoResearch 711-605-152) and alexa-568 donkey anti-goat (Life Technologies A10042). Slices were counterstained with neurotrace 640/660 or 435/455 (Life Technologies N21483 or N21479, respectively). Antibody amplification was not used to visualize eNpHR3.0-eYFP. All images were taken using a Zeiss LSM-710 confocal microscope system.

Cell counting

Confocal images were taken with a 40x objective and z-stacks of approximately 50 μm in depth at a resolution of 256×256. Counting Chr2-eYFP and Arc expressing neurons was performed manually by scrolling through the Z-stack with tiled ROIs. Counting c-fos expressing neurons was performed by creating a projection of the z-stack, and then counting with an automated program written in Labview. It was not possible to count the ChR2-eYFP expressing neurons with the automated program because membrane targeting confounds the detection of cell bodies.

Extended Data

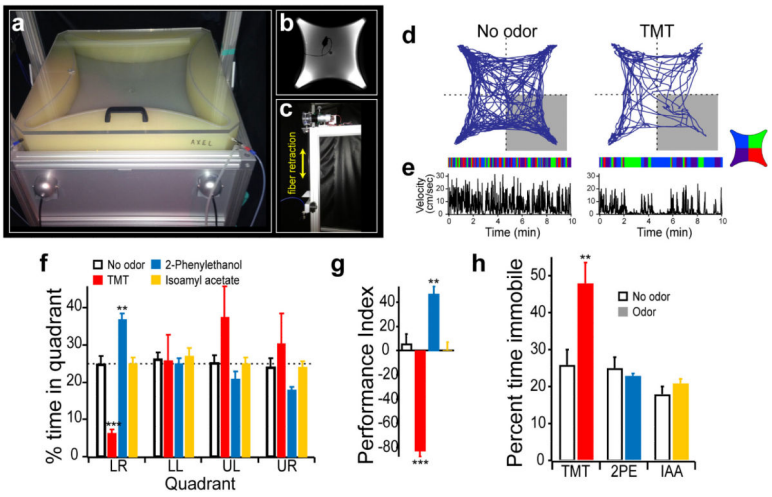

Extended Data Figure 1. Quantification of the four-quadrant behavior assay

a-c, Images of the four-field behavior chamber. **b**, An image, taken from the camera that tracts the position of the animal, shows a mouse tethered to optic fibers that enter the chamber through a port on the left side. **c**, A motorized fiber retraction system adjusts the length of the fiber as the mouse traverses the arena. The trajectory of a representative mouse is plotted for a ten minute period in the absence of odor (left), or following the addition of odor to the lower right quadrant (right). The raster plots below the trajectory graphs represent quadrant occupancy over time. **e**, The velocity over time in the absence of odor (left) or in the presence of TMT (right) reveals bouts of inactivity associated with freezing behavior in the presence of TMT. **f**, The average amount of time spent in each quadrant either in the absence of odor, or the presence of TMT, 2-phenylethanol, or isoamyl acetate. **g**, This quantification is reduced when plotted as the performance index (n=5). **h**, Pauses in locomoter activity are quantified as the percent time immobile in the presence and absence of TMT, 2-phenylethanol, or isoamyl acetate. Immobility is defined as velocity less than 1 cm/sec for at least 1 second. **f-h**, **P < 0.01, ***P < 0.001 paired *t*-test comparing PI with and without odor for each odor group; error bars show SEM.

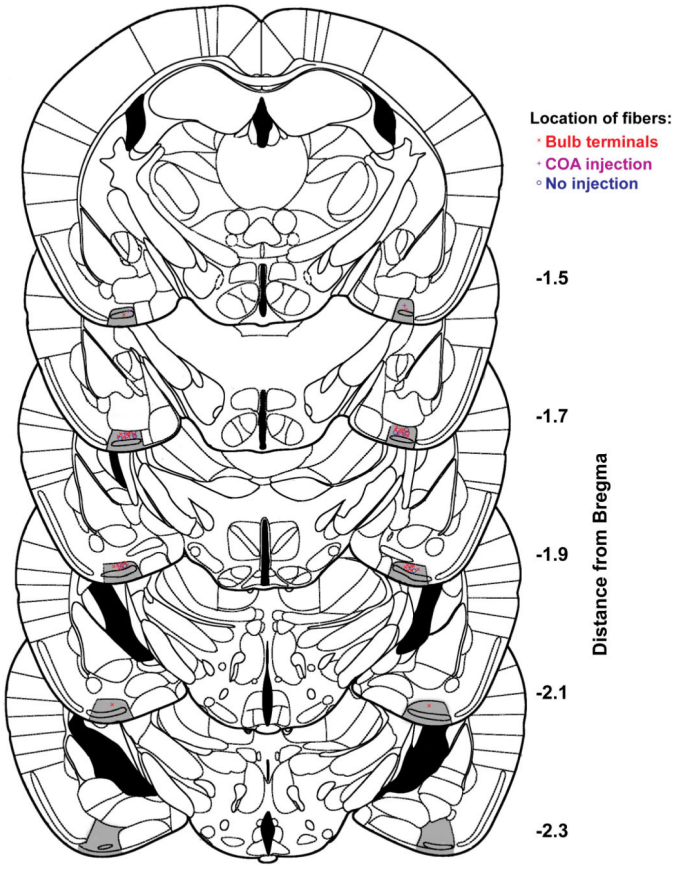

Extended Data Figure 2. Location of optical fibers implanted in cortical amygdala for photoactivation of halorhodopsin

Schematics show coronal sections throughout most of the region containing cortical amygdala. The posterolateral cortical amygdala is highlighted in gray and the location of bilaterally implanted fibers is indicated.

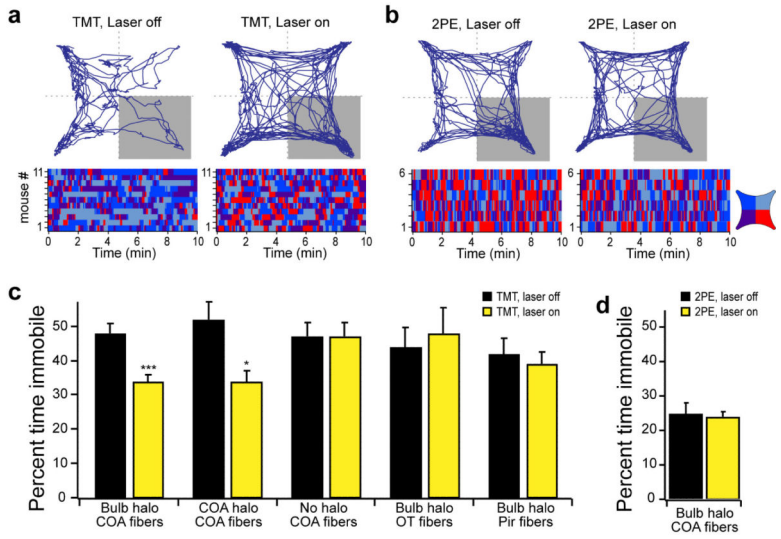

Extended Data Figure 3. Locomotor activity of mice with Optical suppression in cortical amygdala

a,**b** Mice with halorhodopsin in the olfactory bulb and optical fibers in cortical amygdala were optically coupled to a yellow laser and tested in the behavioral assay for the response to TMT (**a**) or 2-phenylethanol (2PE) (**b**) with and without laser stimulation. The position of a representative mouse during a ten minute period in the presence of TMT (**a**) or 2-phenylethanol (**b**) either in the absence (left) or presence (right) of photoactivation during the ten minute behavioral testing. Raster plots show quadrant occupancy over time for each animal (**a**, n=11; **b,** n=6). **c,d**, The percent time immobile in the absence and presence of photoactivation. Immobility is defined as velocity less than 1 cm/sec for at least 1 second. **c**, Response to TMT in mice receiving photostimulation of halorhodopsin in different experimental animals. Bulb halo and COA halo describe mice with halorhodopsin expression in the olfactory bulb and cortical amygdala, respectively. Optical fibers were placed above cortical amygdala (COA, n=11), olfactory tubercle (OT, n=7) or in piriform cortex (Pir, n=8) as denoted below site of injection. Control animals received no viral injection, and fibers implanted into cortical amygdala (n=4). **d**, The percent immobility for mice exposed to 2-phenylethanol in the absence and presence of photoactivation of bulbar axons in cortical amygdala (n=6). **c**,**d**, *P < 0.05, ***P < 0.001 paired *t*-test comparing with and without laser; error bars show SEM.

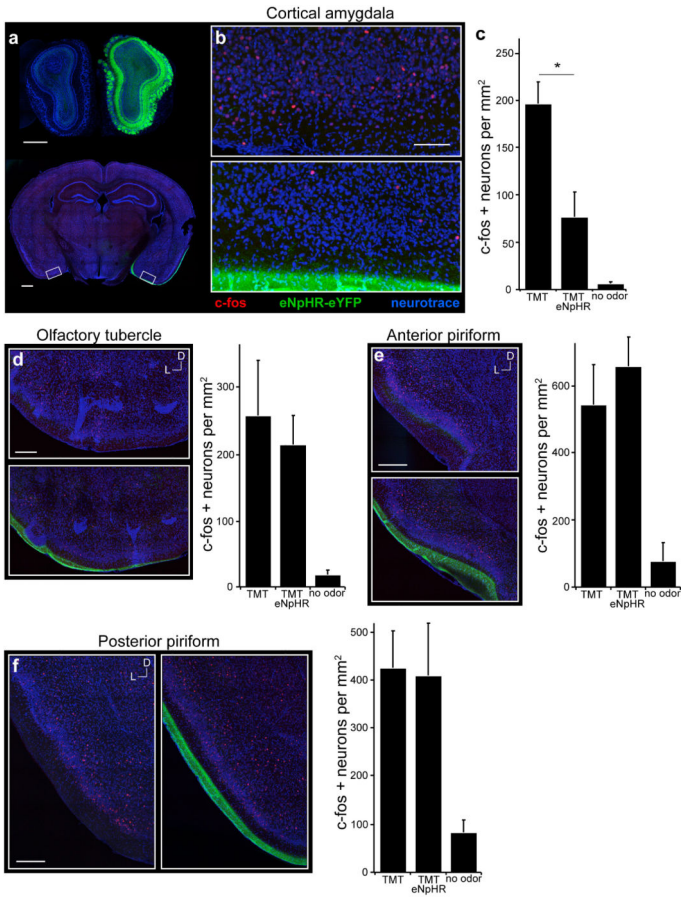

Extended Data Figure 4. Optical suppression of bulbar input to cortical amygdala selectively reduces odor-evoked activity in this region

Mice were unilaterally injected with AAV5-eNpHR3.0-eYFP into the olfactory bulb and exposed to TMT while photoactivating the mitral-tufted cell axon terminals in cortical amygdala. **a**, Coronal section of the olfactory bulbs (top) and of the brain region with cortical amygdala (bottom) reveal halorhodopsin expression in the bulb and the lateral olfactory tract. **b**, Magnified and cropped image showing the cortical amygdala of both sides of the posterolateral cortical amygdala. Region in the bottom image received photoacivation of halorhodopsin in bulbar axon terminals during odor exposure, whereas the contralateral side (top) did not. Scale bars indicate 200 μm (**a**) and 100 μm (**b**). **c**, The number of c-fos positive neurons was counted for each side of the brain (n=4) as well as in control animals that did not receive any stimuli (n=2) across multiple regions of cortical amygdala. Numbers are normalized by area (mm^2) of 100 μm thick sections for comparison between brain areas. *P < 0.05 paired *t*-test comparing with and without laser; error bars show SEM. **d-f**, Coronal sections showing the olfactory tubercle (**d**), anterior piriform (**e**) and posterior piriform (**f**); the region in the bottom images received photoactivation of bulbar axon terminals in the cortical amygdala. Scale bars indicate 200 μm. Bar Graphs show the number of c-fos positive neurons counted for each side of the brain (n=4) as well as in control animals that did not receive any stimuli (n=2). Error bars show SEM. **a-f**, Images are taken from sections at the following AP distances from bregma: −1.7 (**b**), 1.2 (**d-e**), −1.6 (**f**).

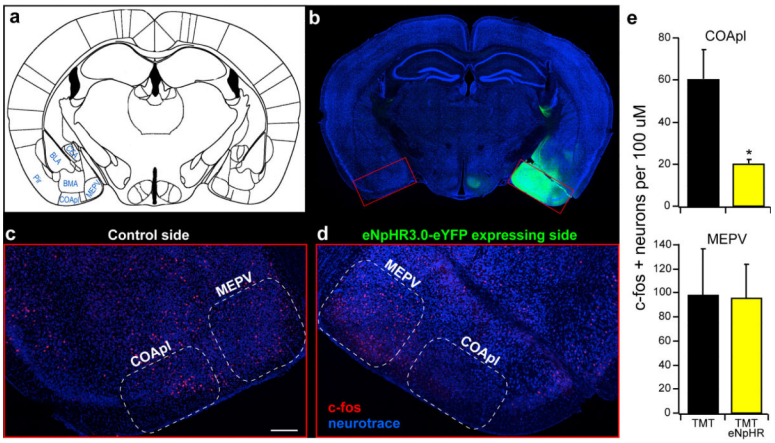

Extended Data Figure 5. Halorhodopsin expression of neurons within cortical amygdala

Injection of AAV into cortical amygdala leads to broad expression of halorhodopsin within cortical amygdala and neighboring areas, however optical silencing is restricted to the cortical amygdala. **a**, Schematic of a coronal section showing cortical amygdala (COApl) in relation to other ventral brain regions. **b-d**, Mice were unilaterally injected with AAV5-eNpHR3.0-eYFP into the cortical amygdala and exposed to TMT while photoactivating halorhodopsin in cortical amygdala neurons. **b**, Coronal section reveals broad expression of halorhodopsin in the cortical amygdala region. This expression is broad covering at least 90% of COApl throughout the anterior-posterior axis. **c-d**, Magnified and cropped image showing c-fos expression in the cortical amygdala. The right side (**d**) received photoactivation during odor exposure , whereas the contralateral side (**c**) did not. Scale bar indicates 200 μm. **e**, The number of c-fos positive neurons was counted for each side of the

brain (n=3) across multiple regions of the cortical amygdala (top) as well as the medial amygdala (MEPV, bottom). The mean cell number for each animal is shown in the bar graph. *P < 0.05 paired *t*-test comparing with and without laser stimulation; error bars show SEM.

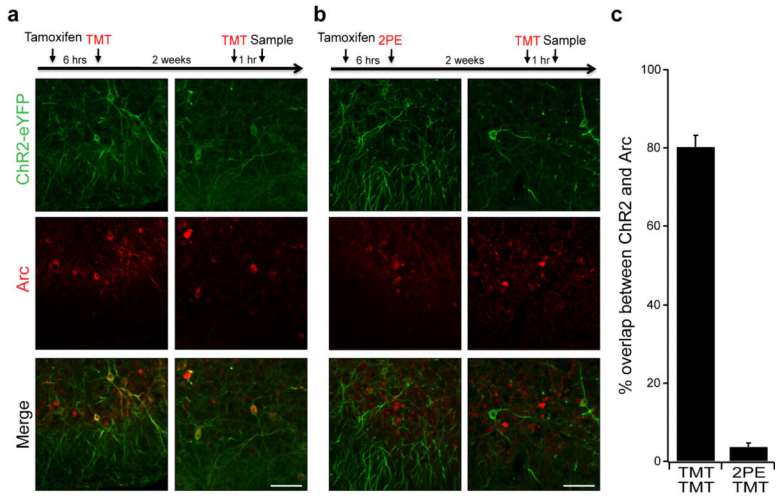

Extended Data Figure 6. The arc promoter can be used to faithfully drive channelrhodopsin expression in odor-specific neurons

Arc-Cre-ER^{T2} mice were administered tamoxifen and exposed to odor to induce ChR2-eYFP expression, and subsequently exposed to either the same odor or a different odor and then sampled for endogenous arc expression. **a**,**b**, The timeline for odor exposure is indicated at the top, and images from two different regions of cortical amygdala are shown from representative animals for each experiment. **a**, TMT exposure induced ChR2-eYFP expression in the cortical amygdala and re-exposure to the same odor induced arc expression detected by immunocytochemistry. **b**, 2-Phenylethanol induced expression of ChR2-eYFP followed by re-exposure to TMT. Scale bar indicates 100 μm. **c**, The number of channelrhodopsin expressing neurons that also express the endogenous arc protein. Neurons were counted across randomly chosen sections throughout the cortical amygdala (n=4).

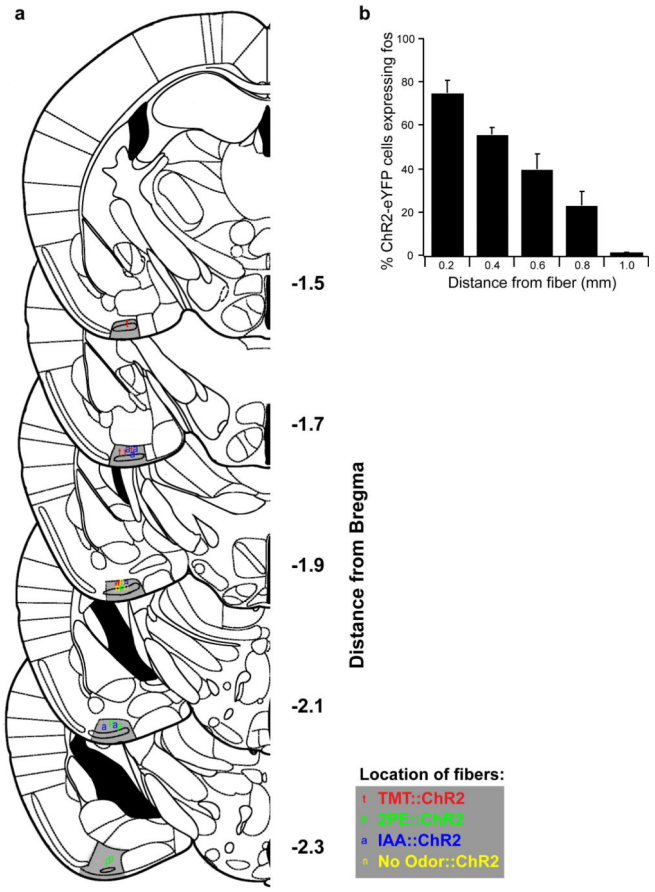

Extended Data Figure 7. Location of optical fibers implanted in cortical amygdala for photoactivation of odor responsive neurons

a, Schematics show unilateral coronal sections throughout most of the region containing cortical amygdala. The posterolateral cortical amygdala is highlighted in gray and the location of unilaterally implanted fibers is indicated. Fibers were not preferentially targeted to one side of the brain, but the fiber positions are collapsed onto unilateral schematics. **b**, The extent of light induced activation of channelrhodopsin expressing neurons as a function of distance from the fiber tip using c-fos expression. ArcCreER^{T2} mice were injected with AAV5-ef1α-DIO-ChR2-eYFP into cortical amygdala, administered tamoxifen and exposed to TMT to induce channelrhodopsin expression. Three weeks later, the cortical amygdala was photoactivated for 10 min with cycles of 30 seconds of pulsed light (10 Hz, 50% duty cycle) and 30 seconds off. Mice were sampled for c-fos immunoreactivity as a function of distance from the fiber tip in 200 μm bins (n=3). $P < 0.001$, one-way Anova; error bars show SEM.

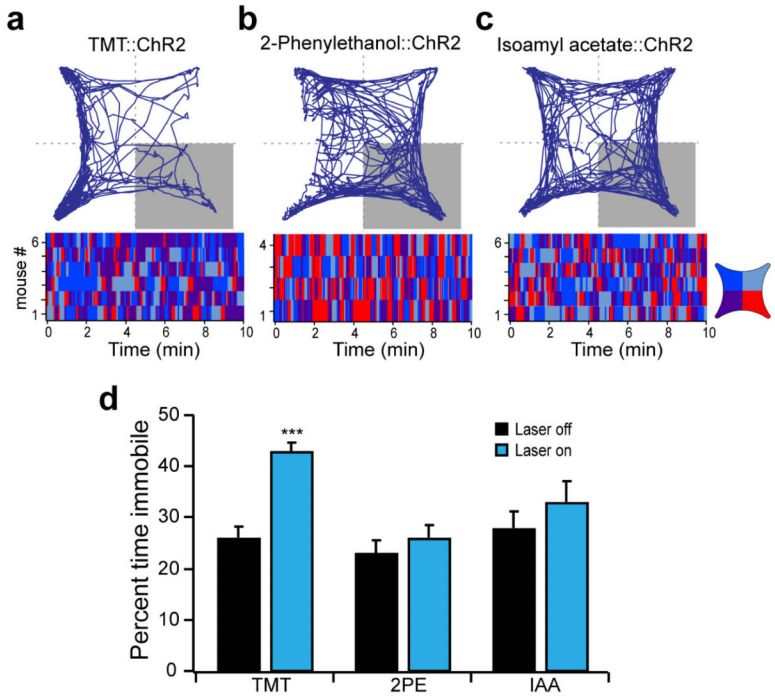

Extended Data Figure 8. Locomotor activity of mice during activation of odor responsive neurons within cortical amygdala

Mice with odor-driven channelrhodopsin expression were tested in the open field assay where they received pulsed photoactivation upon entrance into the lower right quadrant. **a-c**, The trajectory graphs (top) show the position of representative animals with ChR2-eYFP in neurons activated by TMT (**a**), 2-phenylethanol (**b**) or isoamyl acetate (**c**). The raster plots (bottom) show quadrant occupancy over time. **d**, The percent time immobile in the absence and presence of photoactivation. Immobility is defined as velocity less than 1 cm/sec for at least 1 second. **a-c**, TMT (n=6), 2-phenylethanol (n=4) and isoamyl acetate (n=6); ***P < 0.001 paired *t*-test comparing with and without laser; error bars show SEM.

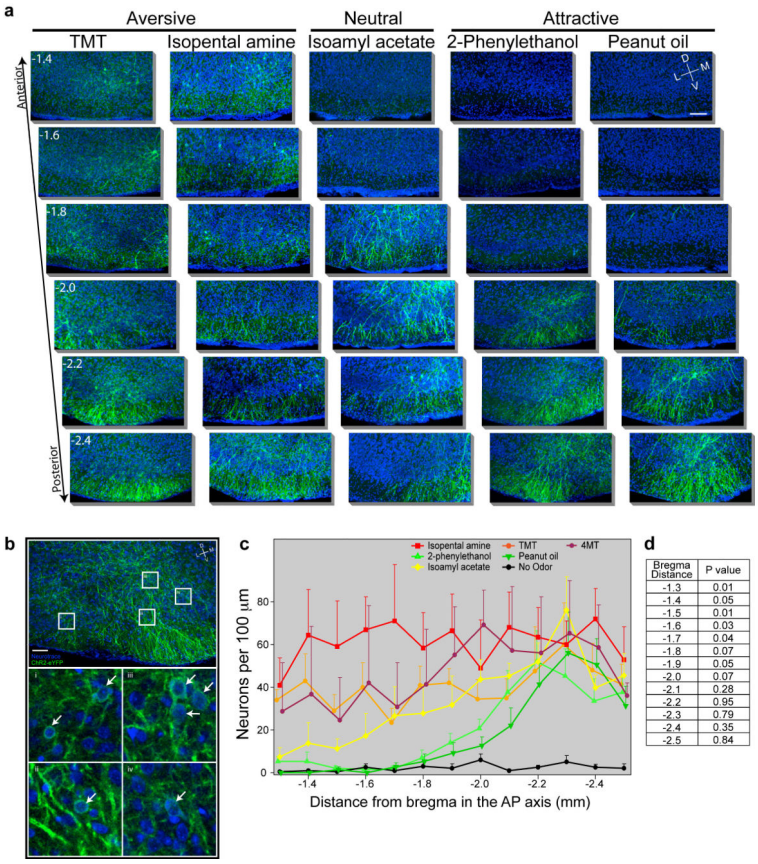

Extended Data Figure 9. The spatial distribution of neurons responsive to different odors within cortical amygdala

a, ArcCreER^{T2} mice were administered tamoxifen and exposed to one of five different odors and then consecutive, serial, coronal sections were collected throughout the cortical amygdala region. Images reveal odor driven ChR2-eYFP expression in serial sections across the cortical amygdala of representative mice for each odor. Images of the ventral brain region are magnified and cropped to show only the posterolateral cortical amygdala, and sections are displayed at 200 µm intervals across 1.2 mm of the anterior-posterior axis. Scale bar indicates 100 µm. **b**, Representative images showing the expression of odor induced ChR2-eYFP with magnified images that reveal identifiable cell bodies for counting. The top image shows a Z-projection of 40 µm through cortical amygdala (left), and the bottom images (i-iv) show magnified single Z-plane images of small areas revealing neuronal cell bodies, indicated by the white arrows. Scale bar indicates 60 µm. **c**, The average number of neurons counted per 100 µm coronal section throughout the posterolateral cortical amygdala for different odors. Error bars show SEM. **c**, A one-way Anova was performed for each point along the anterior-posterior axis, comparing the means between different odors (excluding the no-odor condition). The no-odor condition was compared to each odor at −2.3 from bregma using an unpaired *t*-test; $P < 0.001$ for each odor.

Supplementary Material

Refer to Web version on PubMed Central for supplementary material.

Acknowledgments

We thank L. Abbott, T. Jessell and D. Costantini for critical comments and reading of the manuscript; Bradley Bader for assistance with experiments; Monica Mendelsohn and Nataliya Zabello for help with mice; Phyllis Kisloff for assistance in preparation of the manuscript; and Adriana Nemes and Miriam Gutierrez for general laboratory support. This work was supported by the Howard Hughes Medical Institute and the Mathers Foundation.

References

1. Sosulski DL, Bloom ML, Cutforth T, Axel R, Datta SR. Distinct representations of olfactory information in different cortical centres. Nature. 2011; 472:213–216. doi:nature09868 [pii] 10.1038/nature09868. [PubMed: 21451525]
2. Miyamichi K, et al. Cortical representations of olfactory input by trans-synaptic tracing. Nature. 2011; 472:191–196. doi:nature09714 [pii] 10.1038/nature09714. [PubMed: 21179085]
3. Ghosh S, et al. Sensory maps in the olfactory cortex defined by long-range viral tracing of single neurons. Nature. 2011; 472:217–220. doi:nature09945 [pii] 10.1038/nature09945. [PubMed: 21451523]
4. Stowers L, Logan DW. Olfactory mechanisms of stereotyped behavior: on the scent of specialized circuits. Current opinion in neurobiology. 2010; 20:274–280. doi:10.1016/j.conb.2010.02.013. [PubMed: 20338743]
5. Chamero P, et al. Identification of protein pheromones that promote aggressive behaviour. Nature. 2007; 450:899–902. doi:10.1038/nature05997. [PubMed: 18064011]
6. Nodari F, et al. Sulfated steroids as natural ligands of mouse pheromone-sensing neurons. The Journal of neuroscience : the official journal of the Society for Neuroscience. 2008; 28:6407–6418. doi:10.1523/JNEUROSCI.1425-08.2008 28/25/6407 [pii]. [PubMed: 18562612]
7. Kobayakawa K, et al. Innate versus learned odour processing in the mouse olfactory bulb. Nature. 2007; 450:503–508. doi:nature06281 [pii] 10.1038/nature06281. [PubMed: 17989651]
8. Dewan A, Pacifico R, Zhan R, Rinberg D, Bozza T. Non-redundant coding of aversive odours in the main olfactory pathway. Nature. 2013; 497:486–489. doi:10.1038/nature12114 nature12114 [pii]. [PubMed: 23624375]
9. Li Q, et al. Synchronous evolution of an odor biosynthesis pathway and behavioral response. Curr Biol. 2013; 23:11–20. doi:10.1016/j.cub.2012.10.047 S0960-9822(12)01268-7 [pii]. [PubMed: 23177478]
10. Buck L, Axel R. A novel multigene family may encode odorant receptors: a molecular basis for odor recognition. Cell. 1991; 65:175–187. doi:0092-8674(91)90418-X [pii]. [PubMed: 1840504]
11. Godfrey PA, Malnic B, Buck LB. The mouse olfactory receptor gene family. Proceedings of the National Academy of Sciences of the United States of America. 2004; 101:2156–2161. doi:10.1073/pnas.0308051100. [PubMed: 14769939]
12. Zhang X, Firestein S. The olfactory receptor gene superfamily of the mouse. Nature neuroscience. 2002; 5:124–133. doi:10.1038/nn800. [PubMed: 11802173]
13. Ressler KJ, Sullivan SL, Buck LB. Information coding in the olfactory system: evidence for a stereotyped and highly organized epitope map in the olfactory bulb. Cell. 1994; 79:1245–1255. [PubMed: 7528109]
14. Mombaerts P, et al. Visualizing an olfactory sensory map. Cell. 1996; 87:675–686. [PubMed: 8929536]
15. Vassar R, et al. Topographic organization of sensory projections to the olfactory bulb. Cell. 1994; 79:981–991. [PubMed: 8001145]
16. Rubin BD, Katz LC. Optical imaging of odorant representations in the mammalian olfactory bulb. Neuron. 1999; 23:499–511. [PubMed: 10433262]
17. Gradinaru V, Thompson KR, Deisseroth K. eNpHR: a Natronomonas halorhodopsin enhanced for optogenetic applications. Brain Cell Biol. 2008; 36:129–139. doi:10.1007/s11068-008-9027-6. [PubMed: 18677566]
18. Tye KM, et al. Amygdala circuitry mediating reversible and bidirectional control of anxiety. Nature. 2011; 471:358–362. doi:nature09820 [pii] 10.1038/nature09820. [PubMed: 21389985]

19. Link W, et al. Somatodendritic expression of an immediate early gene is regulated by synaptic activity. Proceedings of the National Academy of Sciences of the United States of America. 1995; 92:5734–5738. [PubMed: 7777577]
20. Boyden ES, Zhang F, Bamberg E, Nagel G, Deisseroth K. Millisecondtimescale, genetically targeted optical control of neural activity. Nature neuroscience. 2005; 8:1263–1268. doi:nn1525 [pii] 10.1038/nn1525. [PubMed: 16116447]
21. Denny CA, et al. Hippocampal memory traces are differentially modulated by experience, time, and adult neurogenesis. Neuron. 2014; 83:189–201. doi:10.1016/j.neuron.2014.05.018. [PubMed: 24991962]
22. Choi GB, et al. Driving Opposing Behaviors with Ensembles of Piriform Neurons. Cell. 2011; 146:1003–1014. doi:Doi 10.1016/J.Cell.2011.07.041.
23. Stettler DD, Axel R. Representations of odor in the piriform cortex. Neuron. 2009; 63:854–864. doi:S0896-6273(09)00684-9 [pii] 10.1016/j.neuron.2009.09.005. [PubMed: 19778513]
24. Poo C, Isaacson JS. Odor representations in olfactory cortex: “sparse” coding, global inhibition, and oscillations. Neuron. 2009; 62:850–861. doi:S0896-6273(09)00397-3 [pii] 10.1016/j.neuron.2009.05.022. [PubMed: 19555653]
25. Illig KR, Haberly LB. Odor-evoked activity is spatially distributed in piriform cortex. The Journal of comparative neurology. 2003; 457:361–373. doi:10.1002/cne.10557. [PubMed: 12561076]
26. Schwabe K, Ebert U, Loscher W. The central piriform cortex: anatomical connections and anticonvulsant effect of GABA elevation in the kindling model. Neuroscience. 2004; 126:727–741. doi:10.1016/j.neuroscience.2004.04.022. [PubMed: 15183521]
27. Tonegawa S, McHugh TJ. The ins and outs of hippocampal circuits. Neuron. 2008; 57:175–177. doi:10.1016/j.neuron.2008.01.005 S0896-6273(08)00036-6 [pii]. [PubMed: 18215616]
28. Tanaka NK, Tanimoto H, Ito K. Neuronal assemblies of the Drosophila mushroom body. The Journal of comparative neurology. 2008; 508:711–755. doi:10.1002/cne.21692. [PubMed: 18395827]
29. Vet, Louise E. M.; J. C. V. L.; Heymans, M.; Meelis, E. An airflow olfactometer for measuring olfactory responses of hymenopterous parasitoids and other small insects. Physiological Entomology. 1983:97–106.
30. Faucher C, Forstreuter M, Hilker M, de Bruyne M. Behavioral responses of Drosophila to biogenic levels of carbon dioxide depend on life-stage, sex and olfactory context. Journal of Experimental Biology. 2006; 209:2739–2748. doi:209/14/2739 [pii] 10.1242/jeb.02297. [PubMed: 16809465]
31. Semmelhack JL, Wang JW. Select Drosophila glomeruli mediate innate olfactory attraction and aversion. Nature. 2009; 459:218–223. doi:nature07983 [pii] 10.1038/nature07983. [PubMed: 19396157]
32. Vo-Dinh, T. Biomedical photonics handbook. CRC Press; 2003.
33. Yizhar O, Fenno LE, Davidson TJ, Mogri M, Deisseroth K. Optogenetics in neural systems. Neuron. 2011; 71:9–34. doi:10.1016/j.neuron.2011.06.004. [PubMed: 21745635]
34. Aravanis AM, et al. An optical neural interface: in vivo control of rodent motor cortex with integrated fiberoptic and optogenetic technology. Journal of neural engineering. 2007; 4:S143–156. doi:10.1088/1741-2560/4/3/S02. [PubMed: 17873414]

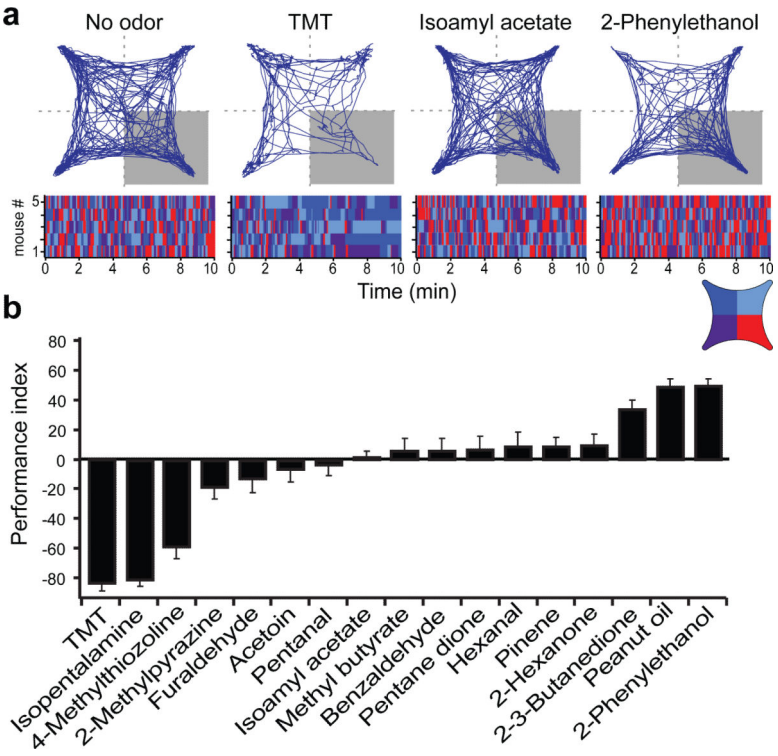

Figure 1. Behavioral assay for innate responses to odor

An open field, 4-quadrant behavioral chamber was used to measure the response to odor delivered in only one quadrant. **a**, The trajectory of a representative mouse is plotted for a ten minute period in the absence of odor or following the addition of odor to the lower right quadrant. The raster plots below the trajectory graphs represent quadrant occupancy over time (x-axis) for each of five different animals. The four colors represent occupancy in each of the four quadrants. Odor was delivered to the lower right quadrant (red). **b**, The average response to an array of odorants is quantified by a performance index that represents the percent difference from chance occupancy in the lower right quadrant (PI = (P-25) /0.25; P = the percent time in the lower right quadrant). One-way anova test, P value < 0.001. n=4-8 for each odor.

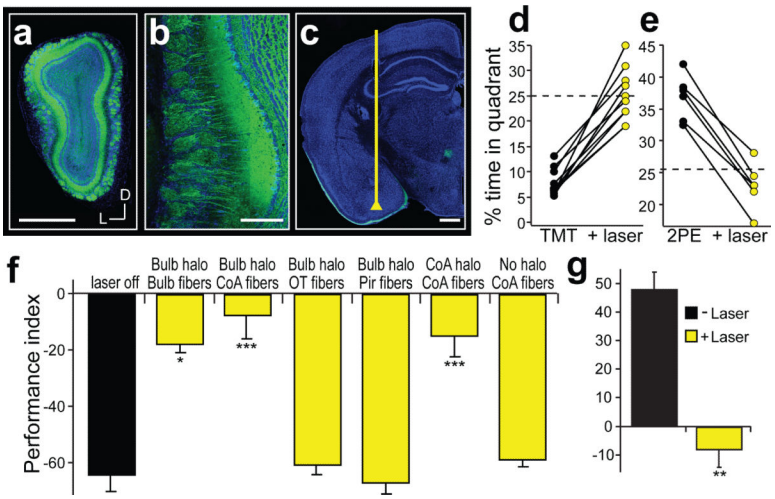

Figure 2. The projections from the olfactory bulb to cortical amygdala are required for innate aversion and attraction to odors

a, Coronal section of a mouse olfactory bulb injected with AAV5-eNpHR3.0-eYFP. **b**, Magnified view of an olfactory bulb showing eNpHR3.0-eYFP expression in mitral cells. **c**, Coronal section depicting the placement of an optical fiber in cortical amygdala, above the axonal output from the olfactory bulb. Scale bar indicates 500 μm (**a**,**c**) and 100 μm (**b**). **d**,e, Mice were optically coupled to a yellow laser and tested in the behavioral assay for the response to TMT (**d**) or 2-phenylethanol (2PE) (**e**) with and without laser stimulation. The percent time each animal spent in the odor quadrant in the absence or presence of photoactivation. **f**, The mean performance index for mice exposed to TMT. The black bar indicates the average response of all mice to TMT in the absence of photoactivation, and the yellow bars indicate responses to TMT with photoactivation for different experimental animals. Bulb halo and CoA halo describe mice with halorhodopsin expression in the olfactory bulb and cortical amygdala, respectively. Optical fibers were placed above the bulb (n=3), cortical amygdala (CoA, n=11), olfactory tubercle (OT, n=7) or in piriform cortex (Pir, n=8) as denoted below site of injection. The last two bars on the right side have either halorhodopsin in the neurons of cortical amygdala (n=5), or receive no viral injection (n=4), and fibers implanted into cortical amygdala. **g**, The mean performance index for mice exposed to 2-phenylethanol in the absence and presence of photoactivation (n=6). **f**,**g**, *P < 0.05, **P < 0.01, ***P < 0.001 paired *t*-test comparing PI with and without laser for each group; error bars indicate SEM.

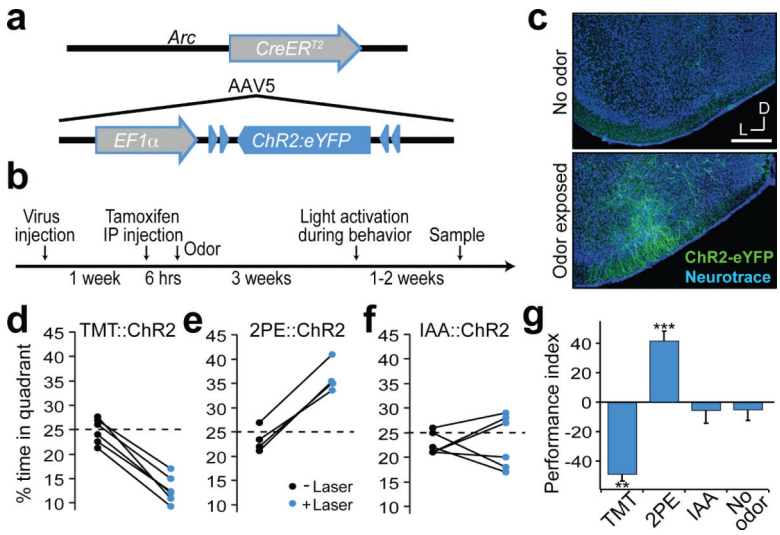

Figure 3. Activation of odor responsive neurons within cortical amygdala is sufficient to recapitulate behavioral responses

a, The genetic strategy used to express ChR2 in odor responsive neurons. The tamoxifen sensitive Cre recombinase, $CreER^{T2}$, was expressed under the control of the promoter of the activity-dependent gene, *arc*, in a transgenic mouse. The gene encoding Cre-dependent ChR2-eYFP was introduced into the cortical amygdala by infection with AAV5. **b**, The timeline for experimental manipulations. The animal was sampled upon termination of behavioral testing. **c**, Representative images showing the expression of ChR2-eYFP in mice that received tamoxifen injection followed by exposure to either the odorant isoamyl acetate (bottom) or no odor as a control (top). Scale bar indicates 300 μm. **d-f**, Mice with odor-driven channelrhodopsin expression were tested in the open field assay where they received pulsed photoactivation upon entrance into one quadrant. The percent time each animal spent in the lower right quadrant in the absence and presence of pulsed photoactivation in mice with neurons activated by TMT (**d**), 2-phenylethanol (**e**) and isoamyl acetate (**f**). **g**, The average performance index for mice receiving photostimulation of neurons activated by TMT, 2-phenylethanol, isoamyl acetate, or no odor, respectively from left to right (n=3-6). **P < 0.01, ***P < 0.001 *t*-test comparing PI with and without laser; error bars indicate SEM.

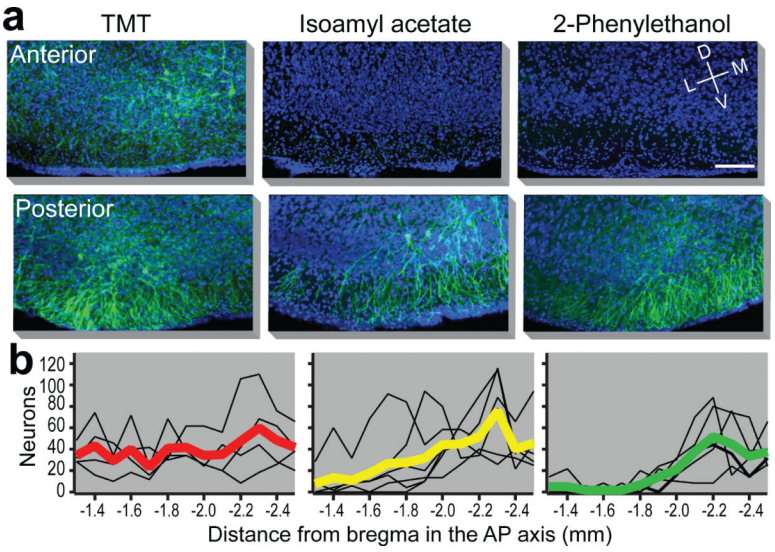

Figure 4. The spatial distribution of neurons responsive to different odors within cortical amygdala

ArcCreER^{T2} mice were administered tamoxifen and exposed to one of three different odors and then consecutive, serial, coronal sections were collected throughout the cortical amygdala region. **a**, Images reveal odor driven ChR2-eYFP expression in representative images of anterior (top) and posterior (bottom) cortical amygdala for each odor. Images of the ventral brain region are magnified and cropped to show only the posterolateral cortical amygdala, and sections are displayed at −1.4 and −2.2 mm relative to bregma. Scale bar indicates 100 μm. **b**, The number of neurons counted per 100 μm throughout the posterolateral cortical amygdala is displayed for each odor. The number for each animal is indicated with a thin black line and the heavier line shows the mean for the odor group (n=4-6).